A NOVEL INTER CORE-CLADDING LITHIUM NIOBATE THIN FILM COATED FIBER MODULATOR/SENSOR

Tracee L. Jamison*[a], Phillip Kornriech[b], Chung Yu[c]
[a]NASA Goddard Space Flight Center, Parts Packaging and Assembly Office, Greenbelt, MD 20771
[b]Syracuse University, Department of Electrical and Computer Engineering, 121 Link Hall, Syracuse, NY 13244
[c]North Carolina A&T State University, Department of Electrical and Computer Engineering, Ron McNair Building, Greensboro, NC 27411.

Keywords: Lithium Niobate, Fiber Modulator/Sensor, Sol gel Fiber, Electrooptic Modulator, Acoustooptic Sensor

ABSTRACT

A fiber modulator/sensor has been fabricated by depositing a lithium niobate sol-gel thin film between the core and cladding of a fiber preform. The preform is then drawn into 125 um fiber. The proposed design of lithium niobate cylinder fibers can enhance the existing methodology for detecting sound waves under water utilizing the acoustooptic properties of lithium niobate. Upon application of a stress or strain, light propagating inside the core, according to the principle of total internal reflection, escapes into the cladding because of the photoelastic boundary layer of lithium niobate. Test results of the lithium niobate fiber reveal a reduction in the 1550 nm, 4mW source with applied tension. The source power from an ordinary quartz fiber under the same stress condition remained invariant to applied tension.

INTRODUCTION

The Lithium Niobate ($LiNbO_3$) Cylinder (LNC) fiber has a 9.6 um diameter borosilicate glass core. The core is surrounded by a 60nm thick layer of $LiNbO_3$ sol-gel, which acts as a highly sensitive photoelastic boundary layer, responding readily to external strain. The $LiNbO_3$ layer is surrounded by a borosilicate glass cladding as shown in Figure 1 whose outside diameter is 125um. When the LNC fiber was tested for its response to applied tension, the signal output decreased with increasing levels of tension while the quartz fiber remained invariant to applied tension.

The response of this fiber to external strain makes it ideal for use as an acoustooptic sensor in under water as well as in deep earth applications[1]. Fibers sensitive to variations in strain in the longitudinal direction are needed in towed array sensor applications.

By directly applying stress or strain to the LNC fiber, the propagation conditions of the guided wave are affected due to the boundary conditions of the fiber being changed.

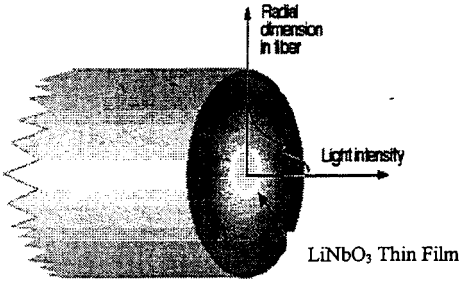

Figure 1. Cross Sectional View of Lithium Niobate Cylinder Fiber

* Tracee.L.Jamison@nasa.gov; phone 1 301 286-1157; fax 1 301 286-9778

METHODOLOGY

A methodology was developed by Dr. Phillip Kornreich of Syracuse University where he deposited a semiconductor thin film material (Cd_3P_2) between the core and cladding of an optical fiber preform and then drew a 125μm fiber using a low temperature fiber drawing technique. This is done by coating a glass rod (fiber core) with a semiconductor thin film, followed by collapsing glass tubes (fiber cladding) around the rod and subsequently making a preform, which is then drawn into fibers. The Semiconductor Cylinder Fibers (SCF) have exhibited gain[2]. A similar approach was utilized to create the LNC fibers.

1. Lithium Niobate Sol-Gel Synthesis

Available as boules, cut crystals or wafers, $LiNbO_3$ single crystal possess an attractive combination of piezoelectric and electrooptic properties which enable it to be widely used as acoustic wave transducers, acoustic delay lines, acoustic filters, optical amplitude modulators, optical phase modulators, second-harmonic generators, Q-switches, beam deflectors, phase conjugators, dielectric waveguides, memory elements, holographic data processing devices, and others[3].

Conventionally $LiNbO_3$ and its related materials are prepared from high-temperature processes, such as single-crystal Czochralski growth, capillary liquid epitaxial technique, Stepanov growth, laser-heated pedestal growth, and so forth[4]. Since $LiNbO_3$ is not a congruently melting compound, the chemical compositions of the single crystals grown from the congruent melt are non-stoichiometric. The solution sol-gel method opens a new avenue for low-temperature processing of $LiNbO_3$. In this regard, using this low-temperature technique reduces direct lithium loss in $LiNbO_3$. As a result, the chemical composition of $LiNbO_3$ is also more controllable.

Sol-gel is a method for preparing metal oxide glasses and ceramics by hydrolyzing a chemical precursor to form a sol and then a gel, which upon drying (evaporation), gives an amorphous oxide. Upon heat treatment crystallization can be induced. The goal of sol-gel processing in general is to control the surfaces and interfaces of materials during the earliest stages of production. The three basic steps of sol-gel processing are:

1. Partial hydrolysis of metal alkoxides to form reactive monomers
2. Polycondensation of these monomers to form colloid-like oligomers (sol)
3. Additional hydrolysis to promote polymerization and cross-linking leading to a 3-D matrix (gel).

The major advantages of the sol-gel approach are

- Lower processing temperatures
- High homogeneity
- High purity
- Multiple metal components can be linked up via oxygen bridging at low temperatures
- Flexibility of the gel network
- Sol-gel process requires no complex or expensive equipment
- Since the network encloses the solvent and is not rigid, it can be casted or molded into various shapes.

The sol is formed by mechanically mixing colloidal particles in waters at a pH that prevents precipitation[5]. The simplest method for preparing multicomponent systems involves making a solution of all the components as alkoxide precursors in a suitable organic solvent and then reacting the solution with water to form the oxide mix. The prime objective in all preparations of multicomponent oxide compositions is to obtain initially a solution of all components in the form of a soluble precursor compound; mixing can then be considered to be at the molecular level and if this level can be retained in the subsequent conversion to oxides, a very homogeneous product should result.

For the LNC fiber, a water/ethanol mixture reacted with a double metal ethoxide precursor, lithium niobium ethoxide ($LiNb(OC_2H_5)_6$, producing amorphous $LiNbO_3$ and an alcohol according to the reaction in [1][6,7,8]. Upon heat treatment, crystalline $LiNbO_3$ formed.

$$LiNb(OC_2H_5)_6 + (3-x/2)H_2O \rightarrow LiNbO_{3-x/2}(OC_2H_5)_x + xC_2H_5OH \qquad [1]$$

2. Fabrication Process of Lithium Niobate Fibers

A glass rod is dipped into amorphous $LiNbO_3$ sol-gel solution and then heat treated to form a thin layer of crystalline $LiNbO_3$. A preform is created by collapsing glass tubes, which form the cladding of the optical fiber, around the core rod coated with crystalline $LiNbO_3$. The collapsing process is done in dual ovens. The resulting cross-sectional area of the LNC fiber preform is approximately 13mm. This preform is then pulled to 125 μm fibers by a low temperature fiber drawing process. The ratio between the preform diameter and the fiber diameter is

$$\frac{\text{Preform Diameter}}{\text{Fiber Diameter}} = 106.347 \qquad [2]$$

This ratio comes from the relationship between the rate the preform feeding mechanism is lowering the fiber preform into the oven at the top of the drawing tower and the rate at which the fiber is being pulled into the capstan at the bottom of the drawing tower. The $LiNbO_3$ crystalline layer is approximately 6.4μm thick when applied around the glass core. According to [2], the resulting film thickness after drawing the fiber will be approximately 60nm. During the fiber pulling process the $LiNbO_3$ film is subject to a pressure of 1000 to 2000 atmospheres. This is similar to the pressure diamonds are subjected to during formation.

ANALYSIS

Light propagates in the LNC fiber according to the principle of total internal reflection (TIR). The diameter of the core of the LNC fiber is 10μm and that of the entire fiber is 125um, while the lithium niobate boundary layer is approximately 60nm. The boundary layer is assumed to have negligible influence on the propagation of light in the core in the absence of strain and doesn't impose a double cladding effect to the fiber. During the presence of strain or stress to the fiber, the strain and field components generate a polarization component ΔP_I along the direction I which result in a leakage of light in the fiber.

The LNC fiber is analyzed using Maxwell's Equations but differs when it comes to the boundary conditions because of the $LiNbO_3$ boundary layer. See Figure 2. The propagation characteristics of the guided wave are obtained by requiring the tangential components of the electric and magnetic-field vectors are continuous across the core-cladding boundary and the radiation condition for fields that extend to infinity[9]. However, since the lowest order TM mode is assumed in this analysis, the radial component of the E-field is affected by the boundary layer and is subject to its influence under stress or strain. The resulting fields in the core and cladding of the LNC fiber, using the TM mode, are

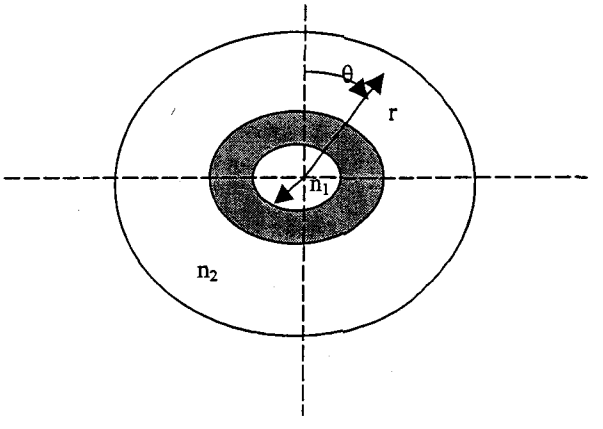

Figure 2. Cross-Sectional View of LNC Fiber

$$H_{\varphi core} = -\hat{a}_{\varphi} u J_1(ur)\left(\frac{j\omega\varepsilon_{core}}{k^2+\omega^2\mu_{core}\varepsilon_{core}}\right)E_{core}e^{j(\omega t-kz)} \quad [3]$$

$$E_{core} = E_{r_{core}} + E_{z_{core}} = [\hat{a}_r k u J_1(ur) - \hat{a}_z(k^2+\omega^2\mu_{core}\varepsilon_{core})J_0(ur)]E_{core}e^{j(\omega t-kz)} \quad [4]$$

$$H_{\varphi clad} = -\hat{a}_{\varphi} w K_1(wr)\left(\frac{j\omega\varepsilon_{clad}}{k^2+\omega^2\mu_{clad}\varepsilon_{clad}}\right)E_{clad}e^{j(\omega t-kz)} \quad [5]$$

$$E_{clad} = E_{r_{clad}} + E_{z_{clad}} = [\hat{a}_r k w K_1(wr) - \hat{a}_z(k^2+\omega^2\mu_{clad}\varepsilon_{clad})K_0(wr)]E_{clad}e^{j(\omega t-kz)} \quad [6]$$

1. Boundary Conditions

Tangential components of the magnetic flux density are continuous across the core-cladding boundary. At r=b, the φ components of magnetic flux density vectors in the core and cladding are equal. Equating equations [3] and [5] results in

$$uE_{core}J_1(ub)\left(\frac{j\omega\varepsilon_{core}}{k^2+\omega^2\mu_{core}\varepsilon_{core}}\right) = wE_{clad}K_1(wb)\left(\frac{j\omega\varepsilon_{clad}}{k^2+\omega^2\mu_{clad}\varepsilon_{clad}}\right) \quad [7]$$

Tangential components of the e-field vector are continuous across the core-cladding boundary; therefore, at r=b, the z components of the e-field across the core-cladding boundary are equal. Equating the z components of equations [4] and [6] result in

$$(k^2+\omega^2\mu_{core}\varepsilon_{core})J_0(ub)E_{core} = (k^2+\omega^2\mu_{clad}\varepsilon_{clad})K_0(wb)E_{clad} \quad [8]$$

The radial components of the e-field vector must be equal across the core-cladding interface, however, in the presence of strain, the difference between the radial components of the electric displacement is equal to ΔP_i; which will be described in Section 2. Taking the difference in the radial components of the e-field in equations [4] and [6], results in

$$[\varepsilon_{core}E_{core}kuJ_1(ub) - \varepsilon_{clad}E_{clad}kwK_1(wb)] = 0 \quad [9]$$

Equation [9] reduces to the conventional equation describing the lowest order TM mode in a step index fiber

2. Polarization Vector ΔP_i

The photoelastic effect[10] involves the first order change in the optical properties of a material medium due to a mechanical strain by a propagating acoustic wave. In this case, we analyze the effects of strain on the thin film layer of $LiNbO_3$. The effect is characterized by a fourth rank tensor p_{idkl}[11], the photoelastic tensor via the relation:

$$\Delta\left(\frac{1}{n^2}\right)_{id} = p_{idkl}S_{kl} \quad [10]$$

where $\Delta\left(\frac{1}{n^2}\right)_{id}$ is a constant for the index ellipsoid[12] and S_{kl}[13] is the shear strain component. The subscripts "id" represent the principal axes of the index ellipsoid. After relating the $\Delta\left(\frac{1}{n^2}\right)_{id}$ to the dielectric tensor ε_{id},

$$\left(\frac{1}{n^2}\right)_{id} = -\frac{\varepsilon'_{id}}{\varepsilon_i \varepsilon_d} \qquad [11]$$

the photoelastic effect is now

$$\Delta\varepsilon_{id} = -\varepsilon_i \varepsilon_d p_{idkl} S_{kl} \qquad [12]$$

In the case of the simultaneous existence of an optical field E and a strain field S_{kl}, then using [13] and [14], we arrive at the polarization induced by the strain in Equation [15].

$$D_i = \varepsilon_{id} E_d = \varepsilon_0 E_i + P_i \qquad [13]$$

Solving for polarization, P_i, from [12] results in

$$P_i = \varepsilon_{id} E_d - \varepsilon_0 E_i = (\varepsilon_{id} - \varepsilon_0 \delta_{id}) E_d \qquad [14]$$

E_d and E_i refer to the electric field in $LiNbO_3$. The polarization induced by the strain is

$$\Delta P_i = \Delta\varepsilon_{id} E_d = \varepsilon_0 \Delta\varepsilon_{id} E_d \qquad [15]$$

and

$$\frac{\Delta P_i}{E_d} = \varepsilon_0 \Delta\varepsilon_{id} \qquad [16]$$

Substituting [16] into [12] results in

$$\Delta P_i = -\frac{\varepsilon_i \varepsilon_d}{\varepsilon_0} p_{idkl} S_{kl} E_d \qquad [17]$$

This equation shows how a strain and field component generates a polarization component, ΔP_i that is proportional to the product $E_d S_{kl}$.

Finally, substituting [17] into [9] results in the new boundary condition.

$$\varepsilon_{core} E_{core} kuJ_1(ur) - \varepsilon_{clad} E_{clad} kwK_1(wr) = -\frac{\varepsilon_i \varepsilon_d}{\varepsilon_0} p_{idkl} S_{kl} E_d \qquad [18]$$

TESTING

The $LiNbO_3$ fiber was tested for its response to various levels of tension applied in the direction of light propagating down the core. Upon application of an external strain the index of refraction of $LiNbO_3$ changes and is related to the dielectric tensor according to [11]. Since $LiNbO_3$ is surrounding the core of the LNC fiber, this change affects the radial

components of the electric field in the core, cladding and thin film layer of $LiNbO_3$. This results in a new boundary condition according to [18].

The fiber under test was an uncoated LNC fiber. A 1550, 4mW light source was connected to a bare fiber adapter, which was used to couple light into the fiber under test. The fiber under test was then housed in a fiber optic cleaver to undergo tension. Light was coupled into the LNC fiber and a Newport Detector detected the power output from the LNC fiber.

The LNC was secured in the cleaver and tension was increased from 100-240. The 1550 laser source was operating during the entire time of testing. The input power was recorded at the beginning of the testing cycle. Once the clamp was secured, the tension was carefully increased from 100-240. Power levels were recorded as a function of applied tension. The result of the testing is illustrated in figures 1 and 2. The LNC fiber results are illustrated in figure 1. A singlemode (SM) uncoated quartz fiber was subjected to the same test conditions. Figure 2 illustrates the results for the standard uncoated single mode fiber.

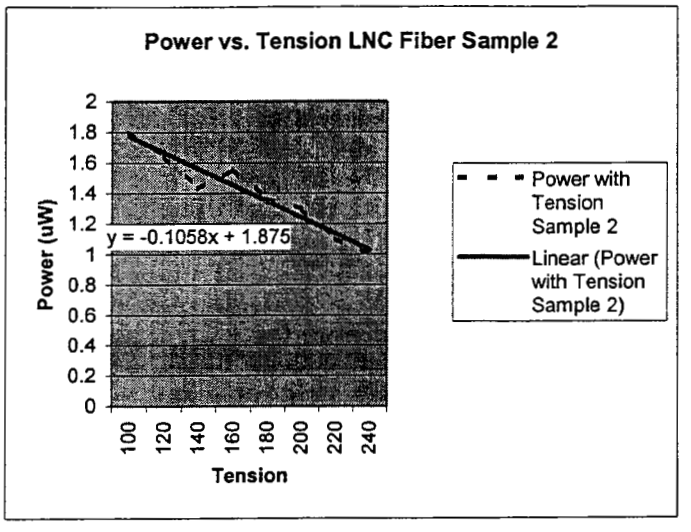

Figure 3. Power Versus Applied Tension for LNC Fiber

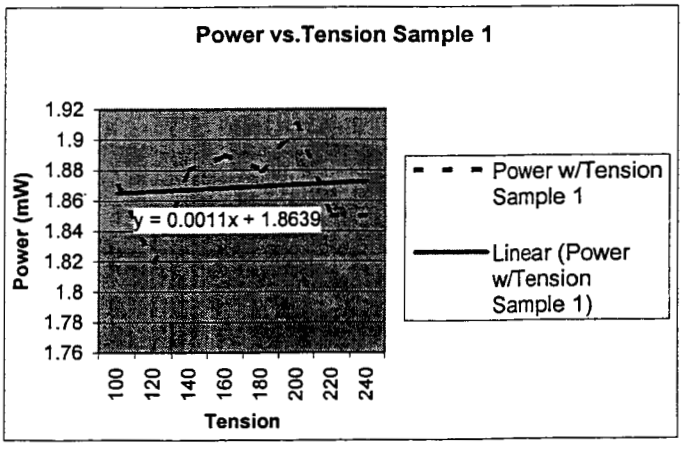

Figure 4. Power Versus Applied Tension for Standard Uncoated SM Fiber

CONCLUSION

The LNC fiber was fabricated with a photoelastic boundary layer of $LiNbO_3$ and subjected to tension testing in order to verify the presence of the layer and its response to stress. The test results suggest the presence of this thin film layer and also its response to applied tension. According to [12], upon application of a mechanical strain to the photoelastic material, the change in the dielectric tensor is negative. This decrease in the dielectric tensor is reflected in the negative slope of Figure 3. The index of refraction, which is related to the dielectric tensor of $LiNbO_3$ is 2.2, which is much greater than that of the glass boundaries surrounding it. Upon application of stress, the index of refraction decreases with applied stress, S_{kl}, in [11] and subsequently, polarization component results, which affects the radial component of the optical field. According to [17], this change is negative, resulting in a decrease in field intensity.

1. Future Applications

The LNC fiber can be configured into a D-shaped fiber with electrodes deposited on the flat surface. See Figure 5. This fiber can then be used as an electrooptic modulator, thereby making it easily integrated into fiber optic networks. Current $LiNbO_3$ thin electrooptic modulators incur 50% losses. Research is currently being done at Syracuse University and NASA Goddard Space Flight Center, to realize this device.

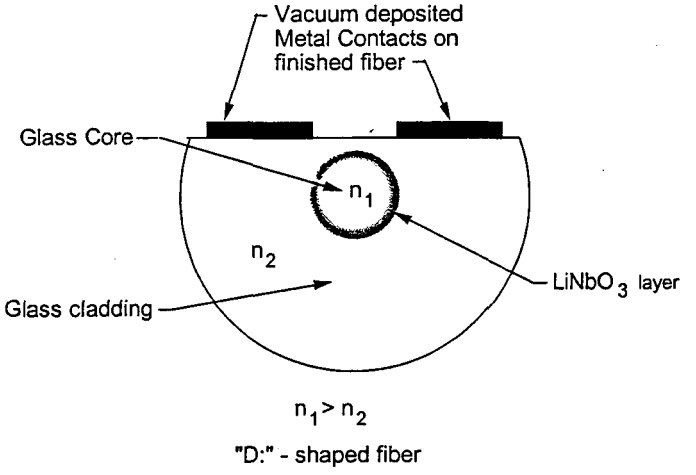

Figure 5. D-Shaped LNC Fiber Design for Electrooptic Modulator

1. Waagard, Ole Henrik, Geir Bjarte Havsgard, Gunnar Wang, "An Investigation of the Pressure-to-Acceleration Responsivity Ratio of Fiber-Optic Mandrel Hydrophones", Journal of Lightwave Technology, **19**, 7, pp. 994-1003, July 2001.
2. Kim, Jin-Sung, J. Flattery, D. Keller and P. Kornreich, "Cd_3P_2 Cylinder Fiber", 4047-18, Aero Sens SPIE Conference 27 April 2000 in Orlando, FL.
3. Weis, R.S., T.K. Gaylord, "Lithium Niobate: Summary of Physical Properties and Crystal Structure", Applied Physics A, **37**, pp. 191-203, 1985.
4 Weis, R.S., T.K. Gaylord, "Lithium Niobate: Summary of Physical Properties and Crystal Structure", Applied Physics A, **37**, pp. 191-203, 1985.
5. Hench, L.L., West, J.K., "The Sol-Gel Process", Chem. Rev, **90**,1, pp. 33-72, Jan-Feb 1990.
6. Hirano, S., and K. Kato, "Formation of $LiNbO_3$ films by Hydrolysis of Metal Alkoxides", Journal of Non-Crystalline Solids **100**, pp. 538-554, 1988.

7. Hirano, Shin-Ichi and Kazumi Kato, "Synthesis of $LiNbO_3$ by Hydrolysis of Metal Alkoxides", Advanced Ceramic Materials, **2**, 2, 1987.
8. Hirano, Shin-Ichi and Kazumi Kato, "Preparation of Crystalline LiNbO3 Films with Preferred Orientation by Hydrolysis of Metal Alkoxides", Advanced Ceramic Materials, **3**, 5, 1988.
9. C.Yeh, "Advances in communication through light fibers", Advances in Communication Systems, vol. 4, Theory and Applications, New York: Academic, 1975.
10 Yariv, Amnon, *Quantum Electronics*, pp. 325-327, John Wiley & Sons, New York, 1989.
11. Nye, J.F, *Physical Properties of Crystals*, Oxford University Press, England, 1957.
12. Ghatak, A.K., Thyagarajan, K. *Optical Electronics*, pp. 87 and Chapter 16, Cambridge University Press, Cambridge, 1989.
[13] Kittel, C, *Introduction to Solid State Physics*, 4th ed, Wiley, New York, 1971.